ELSEVIER

Chemical Geology 203 (2004) 169–179

CHEMICAL GEOLOGY
INCLUDING
ISOTOPE GEOSCIENCE

www.elsevier.com/locate/chemgeo

The nature of melt inclusions inside minerals in an ultramafic cumulate from Adak volcanic center, aleutian arc: implications for the origin of high-Al basalts

Pierre Schiano[a,*], Robert Clocchiatti[b], Pierre Boivin[a], Etienne Medard[a]

[a] *Laboratoire Magmas et Volcans, OPGC-Université Blaise Pascal-CNRS, 5 rue Kessler, 63038, Clermont-Ferrand, France*
[b] *Laboratoire Pierre Süe, CEN Saclay, CEA-CNRS, 91191 Gif-sur-Yvette, France*

Received 6 February 2003; accepted 3 October 2003

Abstract

In order to characterise the parental melts of crustal ultramafic cumulates from arc environments, we have undertaken a study of melt and fluid inclusions in olivine and clinopyroxene crystals in a typical cumulate xenolith from Adak Island, Aleutian Island Arc. The crystals contain inclusions either of silicate melts plus a H_2O-rich bubble or H_2O-dominated fluids, indicating H_2O saturation of the trapped melt during the entire course of its crystallisation. Homogenisation experiments of the silicate melt inclusions give entrapment temperatures ranging between 940 and 1010 °C. After homogenisation, the melt inclusions range in composition from basalt to dacite ; the Al_2O_3 and SiO_2 contents increase from 18.5 to 26.3 wt.% and 47.1 to 56.4 wt.%, respectively, as MgO and FeO decrease from 6.5 to $\sim$ 0.1 wt.% and 6.5 to 0.3 wt.%. The melt inclusions also have high levels of H_2O, $\geq$ 6 wt.%. Comparisons of the compositional trends in the melt inclusion suite with those in experimental multiply-saturated liquids of basalts indicate that the compositional variations in the melt inclusions reflect progressive crystallisation of an olivine + clinopyroxene assemblage similar to the host cumulate xenolith, at pressures $\geq$ 3.0 kbar and H_2O-saturated conditions. A comparison between lavas from Adak Island and the melt inclusion compositions supports the hypothesis that fractional crystallisation at moderate pressures of hydrous mafic basalts generates high-alumina basalt compositions and leaves large volumes of ultramafic cumulate rocks in the crust beneath arc sections.

Keywords: Melt inclusions; High-alumina basalts; Arc volcanism; Adak Island

1. Introduction

Exposed arc crustal sections, zoned ultramafic complexes and xenoliths brought up in magmas provide direct evidence for the presence of mafic and ultramafic rocks in the lower crust beneath arcs (see Wyllie, 1967; Himmelberg and Loney, 1995, and references therein). A large part of these ultramafic rocks are cumulate assemblages of mafic minerals, which as potential complements to arc magmas may give fundamental constraints regarding models for island arc magma evolution. In particular, they preserve information on the earlier stages of magmatic processes, whereas equilibrium assemblages in lavas

* Corresponding author. Fax: +33-4-7334-6744.
E-mail address: schiano@opgc.univ-bpclermont.fr (P. Schiano).

0009-2541/$ - see front matter © 2003 Elsevier B.V. All rights reserved.
doi:10.1016/j.chemgeo.2003.10.001

mainly record shallow-level differentiation processes. In particular, the crystallisation sequence recorded by the ultramafic cumulates is important in solving the controversy about the origin of high-alumina basalts, the most common basalt type in many arc volcanics centers. High-alumina basalts are proposed to be primary magmas generated by high degree melting of subducted oceanic crust (e.g., Marsh, 1976; Myers et al., 1985; Brophy and Marsh, 1986; Myers, 1988) or differentiated magmas formed by crustal-level fractionation dominated by olivine and clinopyroxene from melts of peridotite (e.g., Nicholls and Ringwood, 1973; Perfit et al., 1980; Kay, 1980; Kay and Kay, 1985a; Nye and Reid, 1986; Uto, 1986; Kersting and Arculus, 1994). According to the latter model, ultramafic cumulates in arc centers would represent the necessary crystalline residues to produce high-alumina basalts (Conrad and Kay, 1984; DeBari et al., 1987; Kay and Kay, 1985b). Other hypotheses to the origin of high-alumina basalts have emphasized possible accumulation of plagioclase in less aluminous magmas (Crawford et al., 1987) and extensive interaction of ascending magmas with refractory mantle (e.g., Kelemen, 1990).

Phase equilibria experiments performed under anhydrous conditions on natural high-alumina (low MgO, <6 wt.%) and low-alumina (high MgO, >9 wt.%) compositions have been interpreted to be consistent with both of these hypotheses. Some experiments have postulated an eclogite source (subducted ocean crust) for high-alumina basalts because olivine is not a liquidus phase at any pressure investigated (i.e., high-alumina compositions cannot be derived from peridotites, nor by olivine fractionation from a more primitive melt at high pressure), whereas garnet and/or clinopyroxene are the liquidus phases at high pressure (>25 kbars) (Baker and Eggler, 1983; Johnston, 1986). Conversely, based on high-pressure phase equilibrium data obtained for a high-magnesian composition, Gust and Perfit (1987) have proposed a model in which mantle-derived high-magnesian, low-alumina arc basalts produce high-alumina compositions by fractionation of augite and olivine at pressures less than 10 kbars. Finally, Baker and Eggler (1983, 1987) have shown that plagioclase can be a liquidus phase of high-alumina compositions at 1 atm to 20 kbar pressure, supporting thus a plagioclase accumulation hypothesis.

Also, although aqueous fluids released from subducted oceanic crust are widely believed to play an important part in the genesis of arc basalts, there is still disagreement on the exact role of H_2O in generating high-alumina basalts and influencing their subsequent differentiation. Several authors have postulated that high-alumina basalts have low pre-eruption H_2O contents that cannot significantly affect the overall phase relations (see Johnston, 1986 and references therein). However, others have argued for high H_2O contents in magmas that result in a considerable delay of plagioclase crystallisation and the formation of high-alumina differentiates (Sisson and Grove, 1993a,b; Beard and Lofgren, 1992).

An alternative method to study the composition of melts related to the ultramafic cumulate suites in arc settings is to characterise the compositions of melt inclusions trapped inside the cumulate crystals. As only limited decompression of the inclusion takes place during ascent (Tait, 1992; Schiano and Bourdon, 1999), melt inclusions isolated in crystals may thus provide a record of the evolution of the host magma during growth of the host phases and give an estimate of the volatile content prior to eruption. Some previous studies have reported water-by difference estimates and quantitative measurements of H_2O contents for glass inclusions in olivine phenocrysts from subduction-related volcanoes, suggestive of high H_2O contents in low-MgO, high-alumina liquids (Anderson, 1979, 1982; Sisson and Layne, 1993; Sobolev and Chaussidon, 1996; Roggensack et al., 1996). In the present study, we report major-element compositions in olivine- and clinopyroxene-hosted melt inclusions from a typical cumulate xenolith from Adak Island, Aleutian Island Arc. The results suggest that ultramafic cumulates in arc sections are related to high-alumina, H_2O-rich melts through fractional crystallisation and support a model in which high-alumina basalts are formed by fractionation of more primitive melts under high partial pressure of H_2O.

2. Xenolith and melt inclusion description

The Aleutian Island Arc results from the subduction of the Pacific plate beneath the American plate. The position of the volcanic centers defines four principal arc segments separated by major offsets

and both tholeiitic and calc-alkaline magmatic series occur in volcanoes (Kay et al., 1982). The petrology and geochemistry of xenoliths from Adak Island within the Adreanof segment of the central Aleutian Island Arc have been extensively described elsewhere (Conrad and Kay, 1984; DeBari et al., 1987; Conrad et al., 1983). The xenoliths are found in composite pyroclastic flow units at two Plio-Pleistocene calc-alkaline volcanoes, Mount Adagdak and Mount Moffett. The ADAG81-DR cumulate xenolith was collected from Mount Adagdak and weighs over 60 kg (DeBari et al., 1987). It contains 10-cm scale angular clasts of clinopyroxenite in an olivine-rich matrix displaying a mosaic texture. The two main phases, clinopyroxene ($Wo_{47.1-48.1}$, $En_{45.8-47.0}$) and olivine ($Fo_{85.7-86.4}$), have a narrow range of compositions (Table 1) and often include small chromite crystals. The host lava is a MgO-rich (11.83 wt.% MgO and 15.14 wt.% Al_2O_3, see DeBari et al., 1987), olivine-phyric basalt and is similar in composition to suggested parental magmas in the Aleutians (Kay et al., 1982; Nye and Reid, 1986; Perfit et al., 1980). Arguments based on mineral compositions and textural characteristics have led DeBari et al. (1987) to the conclusion that the ADAG81-DR xenolith is a typical example of the cumulates that formed in a magma chamber beneath the crust–mantle boundary in arc settings.

Table 1
Representative analyses (wt.%) of mineral phases in ADAG81-DR ultramafic cumulate xenolith from Adak Island (Aleutian Arc)

	cpx ($n=7$)	ol ($n=7$)	amph ($n=3$)	amph ($n=3$)	sp ($n=2$)
SiO_2	51.99	40.31	41.60	41.23	0.19
TiO_2	0.24	n.d.	1.08	1.18	0.40
Al_2O_3	3.70	n.d.	14.59	16.49	37.99
FeO	3.82	13.13	7.34	8.98	24.99
MnO	0.08	0.20	0.11	0.00	0.17
MgO	16.14	46.16	16.48	14.91	14.65
CaO	22.86	0.04	11.99	11.46	0.21
Na_2O	0.27	n.d.	2.69	2.16	0.00
K_2O	0.00	n.d.	0.19	0.26	0.00
Cr_2O_3	0.64	n.d.	0.33	0.09	19.72
P_2O_5	n.d.	n.d.	0.09	0.06	0.00
NiO	n.d.	0.14	n.d.	n.d.	n.d.
Sum	99.73	99.98	96.48	96.84	98.36

Primary mineral phases: cpx, clinopyroxene; ol, olivine.
Mineral phases inside melt inclusions: amph, amphibole (pargasite); sp, spinel (hercynite).
n, number of analyses.

The melt inclusions we have identified in the ADAG81-DR xenolith range in size from 20–30 to 80–100 μm and occur in both olivine and clinopyroxene crystals (Fig. 1). They are randomly scattered throughout the host minerals or they occur along healed cleavage or curving fracture planes. Their distribution is typical of primary inclusions formed during growth of their host phase and pseudo-secondary inclusions that enter crystals and are trapped along micro-fractures before the host phases have ceased growing (Roedder, 1984).

The inclusions generally contain quenched glass, H_2O-rich (as verified its laser-Raman spectrum peak at 3500 cm^{-1}; Dubessy, personal communication) liquid + vapor bubbles and "daughter" minerals crystallised from the melt during cooling. "Daughter" phases include small amounts of the host phase that crystallised on the inclusion walls and additional hornblende (pargasite) and spinel (hercynite) crystals precipitated from the residual melt (Table 1). The late character of the "daughter" spinel is illustrated by its complete disappearance during experimental heating of the inclusions (see next section) and also by its absence as an isolated phase inside the host minerals. All host minerals contain inclusions either of silicate glass plus a H_2O-rich bubble or H_2O-dominated (plus CO_2 (1388 and 1287 cm^{-1}), and minor amounts of H_2S (2600 cm^{-1}) and N_2 (2330 cm^{-1}) as verified by laser-Raman analysis; Dubessy, personal communication) fluid (Fig. 1), indicating H_2O-saturation of the trapped melt during the entire course of its crystallisation. Abundant signs of decrepitation of the H_2O inclusions are telltale signs of partial escape of the original fluid at high pressures.

3. Homogenisation experiments and results

In order to record the behaviour of the inclusions upon heating and melting and to estimate the composition of the trapped melt at the time of entrapment, high-temperature experiments were performed with a heating microscope stage (Sobolev et al., 1980), which allows visual monitoring of individual melt inclusions during the experiments. The inclusion contents (glass, gas and crystals) were homogenised

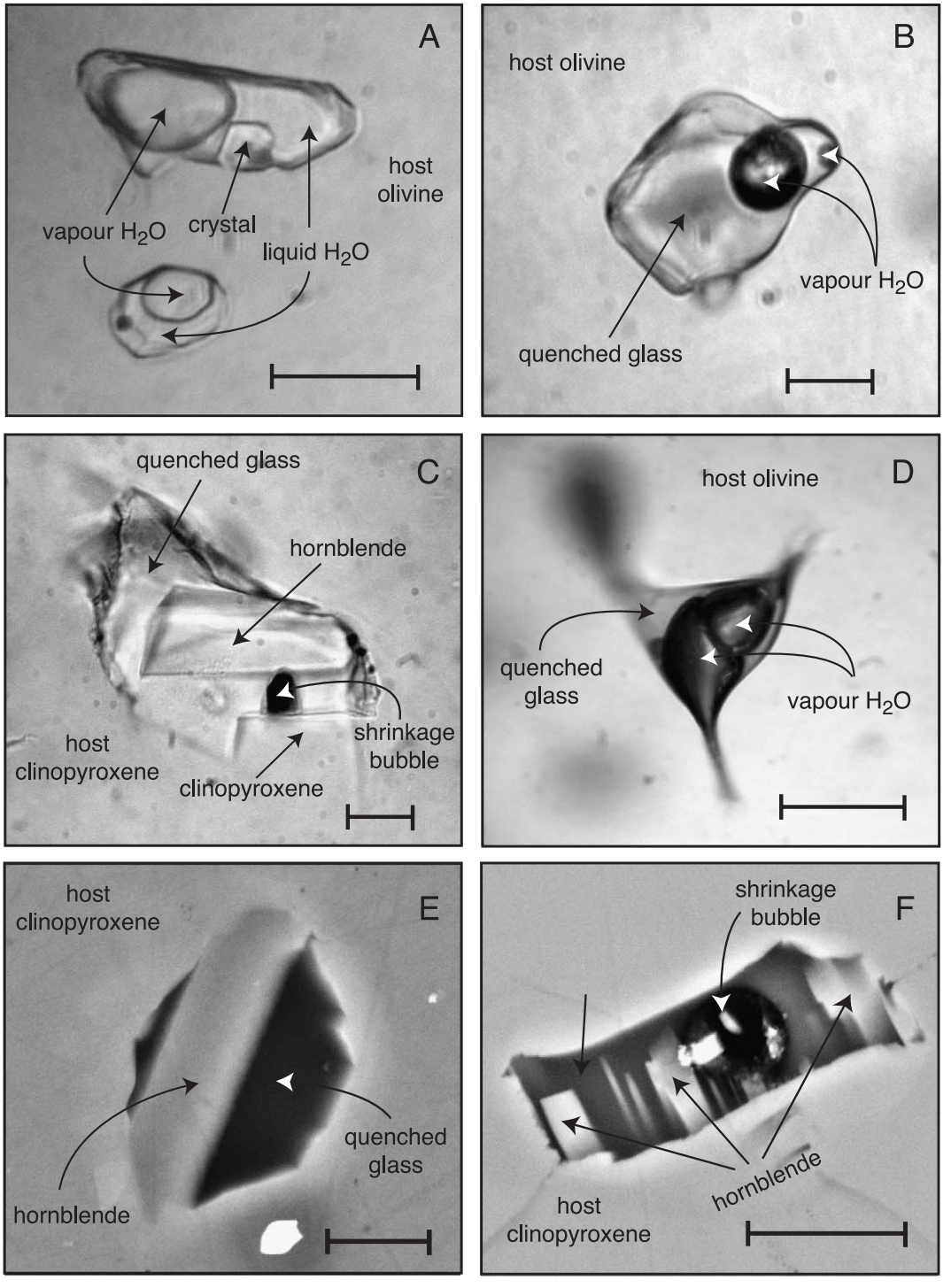
A
host olivine
vapour H_2O
crystal
liquid H_2O
B
host olivine
vapour H_2O
quenched glass
C
quenched glass
hornblende
host clinopyroxene
clinopyroxene
shrinkage bubble
D
host olivine
quenched glass
vapour H_2O
E
host clinopyroxene
quenched glass
hornblende
F
shrinkage bubble
hornblende
host clinopyroxene

Table 2
Representative major-element analyses (wt.%) of homogenised melt inclusions in olivine and clinopyroxene in ADAG81-DR ultramafic cumulate xenolith from Adak Island (Aleutian Arc)

No.	Inc 76	Inc 77	Inc 78	Inc D-5	Inc D-6	Inc C-1	Inc B1-2	Inc A1-2	Inc 66	HL	OK4
SiO_2	53.32	53.23	51.44	47.18	47.42	55.96	56.37	47.06	54.39	48.46	48.97
TiO_2	0.02	0.14	0.62	0.63	0.61	0.02	0.00	0.85	0.33	0.69	0.72
Al_2O_3	26.30	19.48	19.00	18.80	22.70	20.17	20.14	18.52	18.90	15.14	16.27
MnO	0.08	0.18	0.04	0.06	0.14	0.08	0.08	0.12	0.10	0.21	0.18
FeO	0.59	3.05	4.33	5.46	5.12	2.98	0.31	6.45	5.31	9.03	8.78
MgO	≤ 0.05	2.34	5.24	5.56	5.32	0.55	≤ 0.05	6.52	3.00	11.83	9.62
CaO	6.74	9.11	5.96	8.26	8.08	7.58	7.02	10.34	9.22	11.37	12.86
Na_2O	1.05	1.27	1.63	2.20	2.65	3.16	2.24	2.39	1.71	2.08	2.00
K_2O	0.63	0.45	0.81	0.93	0.86	1.01	0.84	0.61	0.31	0.74	0.54
P_2O_5	0.18	0.90	0.03	0.03	0	0.10	0.02	0.03	0.07	n.d.	0.13
Cr_2O_3	0.00	0.07	0.12	0.25	0.24	0.31	0.18	0.25	0.00	n.d.	n.d.
S (ppm)	800	3600	2790	1790	2790	220	1200	1490	840	n.d.	n.d.
Cl (ppm)	1190	1590	1390	1670	1550	3710	1035	1390	660	n.d.	n.d.
Sum	89.18	90.59	89.8	89.77	93.65	92.37	87.53	93.47	93.63	99.55	100.07
Host	$Wo_{47.3}$ $En_{46.5}$	$Wo_{47.0}$ $En_{46.8}$	$Wo_{47.9}$ $En_{46.2}$	Fo_{86}	Fo_{86}	$Wo_{47.4}$ $En_{46.4}$	$Wo_{47.7}$ $En_{45.9}$	Fo_{85}	$Wo_{47.5}$ $En_{46.1}$		
$K_D^{ol/liq}$				0.29	0.29			0.31			
T_h (°C)	940	960	980	990	970	950	940	1010	950		
Normative composition											
Qz	34.2	24.5	18.6	3.5	1.3	17.0	28.6	0.0	18.6	0.0	0.0
Co	13.5	2.7	5.2	0.0	2.9	0.4	3.3	0.0	0.0	0.0	0.0
Or	4.2	2.9	5.3	6.1	5.4	6.4	5.7	3.9	2.0	4.4	3.2
Ab	9.9	11.9	15.4	20.7	23.8	28.9	21.6	21.6	15.5	16.8	16.9
An	36.1	43.5	32.6	43.0	42.6	40.0	39.6	40.6	45.9	29.8	33.8
Di	0.0	0.0	0.0	1.9	0.0	0.0	0.0	11.3	2.0	21.6	23.8
Hy	0.1	6.4	14.5	14.7	14.1	1.5	0.0	11.1	7.4	0.0	2.2
Ol	0.0	0.0	0.0	0.0	0.0	0.0	0.0	2.3	0.0	25.3	18.6
Ne	0.0	0.0	0.0	0.0	0.0	0.0	0.0	0.0	0.0	0.5	0.0

The compositions of the host lava HL (DeBari et al., 1987) and primitive Aleutian lava OK4 from Okmok volcano (Kay et al., 1982) are also reported.
Normative compositions are calculated assuming $Fe^{3+} = 0.15\Sigma Fe$. Qz = quartz, Co = corundum, Or = orthoclase, Ab = albite, An = anorthite, Di = diopside, Hy = hypersthene, Ol = olivine. T_h (°C), temperature at which the inclusion content (glass, gas and crystals), is homogenised. Fe–Mg exchange coefficient $K_D^{ol/liq} = (X_{Fe}^{ol} X_{Mg}^{liq})/(X_{Mg}^{ol} X_{Fe}^{liq})$.

by heating the host crystal in a vertical $Pt_{90}Rh_{10}$ tube, at redox conditions corresponding to the iron–wustite buffer in a purified He atmosphere. The accuracy of the temperature measurements was around ± 5 °C and the system was calibrated at the melting temperatures of Ag (961 °C) and Au (1064 °C). Kinetic runs were performed with a range of heating rates and exposure times in order to assess the effects caused by variations in the rate of melting of the enclosed crystalline phases. The optimal experimental conditions ensuring equilibration during homogenisation of the inclusions correspond to heating rates of 0.87 °C s^{-1} from 20 to 900 °C and 0.47 °C s^{-1} for T>900 °C. With respect to the stability of the host phase, the homogenisation temperature (T_h, the temperature of disappearance of the shrinkage bubble) is also a

Fig. 1. Transmitted light photomicrographs (A, B, C and D) and SEM backscattered electron images (E and F) of silicate melt inclusions (containing quenched glass, H_2O-rich bubbles and "daughter" minerals crystallised from the melt during cooling) and H_2O-rich (liquid + vapour) fluid inclusions in olivine and clinopyroxene crystals from ADAG81-DR cumulate xenolith from Adak Island (Aleutian Island Arc). Bar scale is 20 μm.

minimum estimate of the entrapment temperature of the melt inclusion at the internal pressure. T_h varies between 970 and 1010 °C for olivine-hosted melt inclusions and between 940 and 980 °C for clinopyroxene-hosted melt inclusions. These results are consistent with the equilibration temperatures (980–1030 °C) for the ADAG81-DR xenolith given by the olivine–spinel geothermometer (DeBari et al., 1987). After quenching, the samples were polished to expose the inclusions for electron microprobe analyses.

Homogenised olivine- and clinopyroxene-hosted melt inclusions were analysed for major-elements (Table 2) with a Cameca SX 50 electron microprobe at the Camparis Center (University of Paris VI, France), using an accelerating voltage of 15 keV, sample current of 10 nA. The beam was defocussed for glass analyses, so that Na loss would be reduced. To reduce further Na loss, Na was analysed first with different counting times. The inclusions range in composition from corundum- and quartz-normative, basalt to dacite; major-element variations in these glasses are illustrated in Fig. 2. The most Al_2O_3- and SiO_2-rich inclusions are in clinopyroxenes and the most Al_2O_3- and SiO_2-poor inclusions are in olivines. The Al_2O_3 and SiO_2 contents increase from 16.7 to 26.3 wt.% and 47.6 to 56.0 wt.% respectively, as MgO decreases from 7.3 to ≤ 0.5 wt.%. The glass inclusions also have high levels of volatile elements (predominantly H_2O as verified by laser-Raman analysis), ≥ 6 wt.% based on the low totals of analyses.

4. Discussion

Study of major-element composition of melt inclusions in ADAG81-DR xenolith from Adak Island shows that liquids with very high Al_2O_3 contents can be preserved in ultramafic cumulates in the crust beneath arc sections. In the following, we evaluate the origin of the compositional variations recorded by the inclusions and investigate inferences that can be derived from the data on models for high-alumina basalt genesis.

Overall, the melt inclusion data define a coherent trend on variation diagrams (Fig. 2), suggesting a common origin. They record a decrease in MgO with

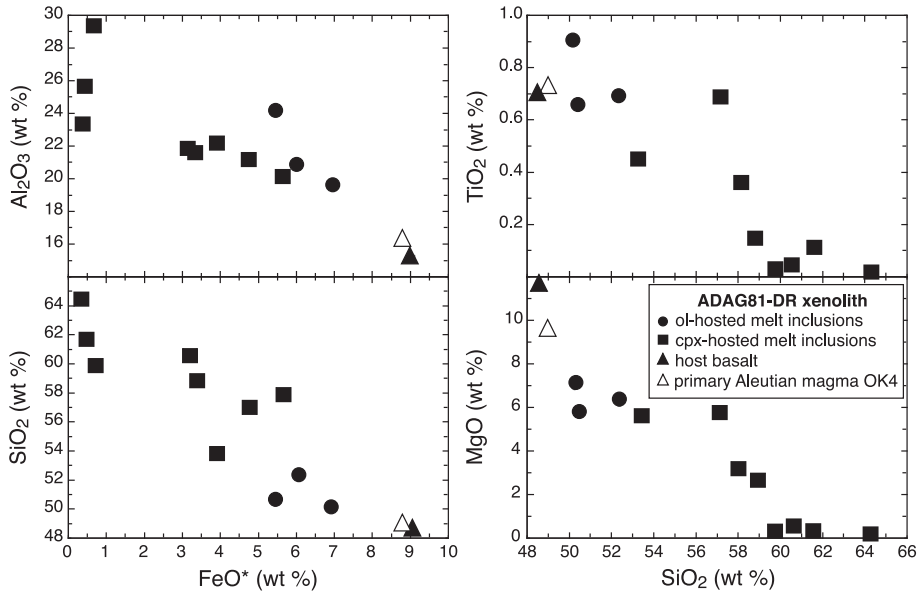

Fig. 2. Major-element variation diagrams for melt inclusions in olivine and clinopyroxene crystals from ADAG81-DR cumulate xenolith. Also shown for comparison are the compositions of the host lava (DeBari et al., 1987) and primitive Aleutian lava OK4 from Okmok volcano (Kay et al., 1982). FeO* is total iron reported as FeO. Major-element concentrations have been recalculated on an anhydrous basis (i.e., normalized to 100%).

increasing SiO_2, Al_2O_3 and decreasing CaO and FeO, consistent with fractionation of an initially mafic liquid by progressive crystallisation of olivine and clinopyroxene. Melt inclusions forming the primitive end of the array in Fig. 2 are thus likely to represent parental melts from which more evolved magma compositions are derived by crystal fractionation, leaving a crystalline residue comparable to the host cumulate assemblage. However, they cannot be identified as *primary* mantle magmas (i.e., unmodified partial melts of mantle wedge source regions) because forsterite values of the host olivines (Fo_{86}) and FeO/MgO ratios (~ 1.0) of the olivine-hosted melt inclusions do not indicate equilibrium with mantle peridotite. We have thus also plotted in variation diagrams of Fig. 2 the compositions of the MgO-rich host lava of ADAG81-DR xenolith (considered by DeBari et al., 1987 as a potential parental magma for the Adak xenolith suites) and a previously postulated primary magma for the Aleutian arc (OK4 tholeiitic basalt from Okmok volcano, see Conrad and Kay, 1984; Kay et al., 1982). In most variation diagrams, the two whole rocks fall on an extension of the compositional trend defined by the melt inclusions.

The compositions of the melt inclusions and experimentally determined multiply-saturated liquids of basalts at 0.5–3 kbar under H_2O-saturated conditions (Sisson and Grove, 1993b; Beard and Lofgren, 1992; Blatter and Carmichael, 2001; Hirose, 1997) have been compared on pseudoternary diagrams in the model system $CaO–MgO–Al_2O_3–SiO_2$ (CMAS). Fig. 3 shows the compositions (recalculated to equivalent CMAS following the procedure of O'Hara, 1968) projected from diopside onto the forsterite–anorthite–quartz plane (Fig. 3a) and from forsterite–quartz onto the perpendicular, best-fit $(forsterite)_2(anorthite)_8$–quartz–diopside plane (Fig. 3b). Anhydrous 7 kbar (Presnall et al., 1979) and H_2O-saturated 15 kbar (Kushiro, 1974) liquidus phase relations of the system forsterite–anorthite–silica are also shown to illustrate the effect of H_2O to reduce the liquidus volume of plagioclase and expand the volume of olivine and pyroxene (e.g., Yoder and Tilley, 1962).

When plotted in the forsterite–anorthite–quartz projection (Fig. 3a), the primitive end of the array of melt inclusion composition plots near the anorthite–forsterite join and the general trend of the melt inclusions with advancing fractionation is one of increasing quartz components. However, Fig. 3b shows that the melt inclusion array extends in fact across the forsterite–anorthite–quartz plane with the primitive end of the array above this plane (i.e., in the diopside-rich side of the $(forsterite)_2(anorthite)_8$–quartz join). In this projection, the general trend with advancing fractionation is one of decreasing diopside component.

As a whole, there is a good agreement between the composition of melt inclusions and hydrous experimental liquids in the two projections albeit the melt inclusion trend extends toward the diopside-poor side of the $(forsterite)_2(anorthite)_8$–quartz join in Fig. 3b. This similarity in composition and the petrographical evidence for water-saturation of the melt inclusions (see Section 2 and Fig. 1) indicate that the compositional variations in the melt inclusions are likely to reflect a fractionation relationship under moderate pressure H_2O-saturated conditions. Accordingly, the range of temperatures found experimentally (900–1100 °C) is in agreement with T_h temperatures (940–1010 °C) for the melt inclusions and olivine–spinel equilibration temperatures (980–1030 °C, see DeBari et al., 1987) for Adak xenoliths. Moreover, the nature of the host and "daughter" phases suggests that the melts trapped inside the inclusions could first crystallise olivine and clinopyroxene in the temperature range of 940–1010 °C, giving way to hornblende precipitation at lower temperatures. Hence, plagioclase cannot crystallise from the H_2O-saturated melt inclusion compositions over the investigated $P–T$ range. This observation together with the stability limits of plagioclase inferred from saturation assemblages of the experimental H_2O-saturated liquids restrict the pressures of the melt inclusions to greater than 2–3 kbar. Note that this conclusion applies not only to the melts associated with ADAG81-DR xenolith but also to those associated with the whole cumulate xenolith series (dunites, wehrlites, clinopyroxenites and hornblendites,) (Conrad and Kay, 1984; DeBari et al., 1987) from Adak Island.

Also, it is important to note that the fractionation trend defined by the melt inclusions is characterised by a decrease in FeO and an increase in SiO_2 with advancing differentiation (Fig. 2). This early iron depletion is a typical feature of the calc-alkaline differentiation trend found at island arc and continental convergent margin volcanoes (Miyashiro, 1974).

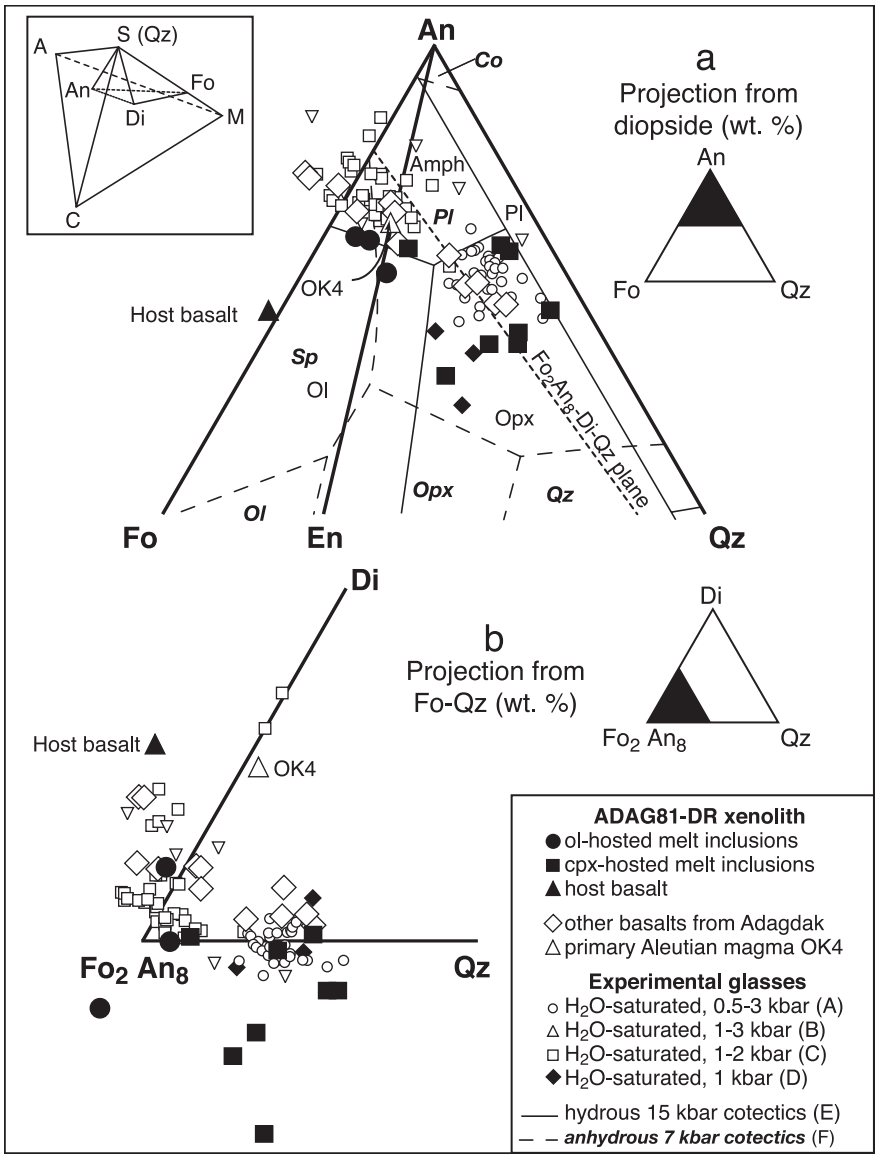

Fig. 3. Comparison of the composition of melt inclusions in ADAG81-DR xenolith, the host lava (Conrad and Kay, 1984) and other whole rocks from Mount Adagdak volcano (Marsh, 1976; Myers et al., 1985; Kay and Kay, 1985a; DeBari et al., 1987; Coats, 1952; Myers and Frost, 1994), and primitive Aleutian lava OK4 (Kay et al., 1982) with experimentally determined liquids at 0.5–3 kbar under H_2O-saturated conditions (A, Blatter and Carmichael, 2001; B, Beard and Lofgren, 1992; C, Sisson and Grove, 1993b; D, Hirose, 1997) in the model system CaO–MgO–Al_2O_3–SiO (CMAS). Symbols are given in the accompanying legend. An = anorthite, Fo = forsterite, En = enstatite, Qz = quartz, Di = diopside, Co = corundum, Pl = plagioclase, Amph = amphibole, Sp = spinel, Ol = olivine, Opx = orthopyroxene. (a) Projection from Di onto the Fo–An–Qz plane. Anhydrous 7 kbar (E, Presnall et al., 1979) and H_2O-saturated 15 kbar (F, Kushiro, 1974) liquidus phase relations are shown for reference. Also reported is the mark of the perpendicular, best-fit Fo_2An_8–Di–Qz plane used in Fig. 3b. (b) Projection from Fo–Qz onto the Fo_2An_8–Qz–Di plane. Analyses have been recast into the CMAS system by following the procedure used by O'Hara (1968). All oxides are in molecular proportions. (insert) relationships of planes and projection points in the CMAS system.

Our results thus support previous models (e.g., Sisson and Grove, 1993b) in which suppression of the Fe-enrichment that characterises the tholeiitic differentiation trend (Fenner, 1931) is related to H_2O-saturation conditions and relevant fO_2.

Analyses of whole rocks (basalts to dacites, with SiO_2 and Al_2O_3 contents ranging from 48.4 to 65.0 wt.% and 15.1 to 19.5 wt.%, respectively, see (Marsh, 1976; Myers et al., 1985; Kay and Kay, 1985a; DeBari et al., 1987; Coats, 1952; Myers and Frost, 1994) from Mount Adagdak volcano are plotted in the pseudo-ternary diagrams of Fig. 3. Like ADAG81-DR melt inclusions, most whole rock lavas define a single trend consistent with the compositions of experimental liquids produced in H_2O-saturated melting experiments on basalts at 0.5–3 kbar. The close correspondence between the erupted lavas and experimental, multiply-saturated hydrous melt compositions supports the hypothesis that the magmas were once multiply-saturated liquids with high H_2O contents. Sisson and Grove (1993a) have calculated that high-alumina basalts should contain at least 6 wt.% H_2O to exist as multiply-saturated liquids at crustal pressures and temperatures ranging between 950 and 1000 °C. On the other hand, the MgO-rich host lava of the xenolith (and the primitive Aleutian lava OK4) falls clearly away from the primitive end of the compositional array defined by the melt inclusions in Fig. 3. The host lava plots toward higher forsterite content than the left end of the compositional array in Fig. 3a and is slightly displaced toward the diopside apex in Fig. 3b. An explanation of this feature is to envision an early episode of crystallisation, by which residual liquids arrive at the silica-poor side of the melt inclusion array ; subsequent fractionation of the host cumulate assemblage can yield the rest of the compositional trend. Alternatively, the olivine-phyric character of the host lava (DeBari et al., 1987) could reflect a selective accumulation of olivine phenocrysts, and therefore, the MgO-rich basalts used for the melting experiments shown in Fig. 3 (e.g., basalt 79–35g from Medicine Lake volcano, California (Sisson and Grove, 1993b) and basalt AT-4 from Atka in the Aleutians (Beard and Lofgren, 1992)) would provide more adequate parental magma compositions for the Adagdak whole rock series.

As shown in Fig. 3, melt inclusions and Mount Adagdak whole rocks have close compositions. However, melt inclusions have generally higher Al_2O_3 contents and thus corundum-normative compositions. Compositional differences between melt inclusions and their host lavas have been observed previously and in a variety of settings (e.g., Sobolev and Shimizu, 1993; Clocchiatti et al., 1998). In these cases, melt inclusions have been interpreted as sampling a range of liquids (reflecting a range of extents of melting, and/or melting processes) trapped before mixing and homogenisation in magma chambers diluted or averaged them to produce the compositions of erupted lavas.

It should also be noted that, although there is a good agreement between H_2O-saturated melt inclusions and the most alumina-rich whole rock compositions (Fig. 3), they are distinguishable by their coexisting mineral assemblages; i.e., whole rock lavas are characterised by abundant plagioclase (ranging from An_{90} in the more basic basaltic andesites to An_{70} in the most differentiated andesites, see Marsh, 1976). Taken together, these observations are consistent with a model of coupled fractionation and decompression, similar to that proposed by Beard and Lofgren (1992). At crustal pressures and temperatures around 1000 °C, high-alumina basalt compositions are generated by fractionation of mafic phases from low-alumina, H_2O and MgO-rich magmas, leaving crystalline residues similar to the cumulate rock series observed in xenoliths found in lavas of Adak Island. Such evolution is mainly governed by the presence of high contents of H_2O, which delays plagioclase crystallisation by lowering its stability limit, thus increasing the proportion of early crystallising mafic phases and driving residual liquids to high Al_2O_3 contents. As they ascend to lower pressure, magmas become water-saturated, exsolve H_2O and crystallise abundant plagioclase phenocrysts (Beard and Lofgren, 1992). This model is supported by the occurrence in the more primitive whole rock–lavas of Mount Adagdak of calcic plagioclase (An_{90}), which is consistent with high magmatic H_2O contents (Arculus and Wills, 1980; Sisson and Grove, 1993b).

5. Conclusion

The identification of H_2O-saturated, high-alumina melt inclusions trapped in olivine and clinopyroxene crystals in an ultramafic xenolith from Adak Island

supports the fractionation model developed for high-alumina Aleutian lavas (Conrad and Kay, 1984; Kay and Kay, 1985b). Moderate pressure fractional crystallisation of hydrous mafic basalts in the crust beneath arcs leads to the formation of more evolved high-alumina basalts and leaves a cumulate rock series similar to that observed in zoned Alaskan-type ultramafic complexes (Wyllie, 1967; Himmelberg and Loney, 1995) and plutonic xenoliths in lavas from Aleutian volcanoes (Conrad and Kay, 1984; DeBari et al., 1987). Recognising that high-alumina basalt compositions dominate many arc systems, a possible consequence of such crystallisation processes is the addition in the crust of large volume of ultramafic crystalline residues (Kay and Kay, 1985b), which would shift the lower crust toward more mafic compositions. Moreover, it has been recently proposed that these ultramafic crustal cumulates could provide plausible sources of the calcic, silica-undersaturated primary magmas recently identified in arc environments (Schiano et al., 2000).

Acknowledgements

Financial support was provided by grants from INSU-CNRS (“Intérieur de la Terre”. program) and the European Community’s Human Potential Programme under contract HPRN-CT-2002-00211, (Euromelt). We thank J. Dubessy for the Raman spectrometry analyses and A. Grunder for the discussions. Reviews by T.W. Sisson, I.A. Sigurdsson and two anonymous reviewers have improved the manuscript. SEM backscattered electron images were done at “service de microscopie électronique”, UFR 928, Paris VI, with assistance from Mr. Boudouma. R.W. Kay supplied the nodule. **[CA]**

References

Anderson Jr., A.T., 1979. Water in some hypersthenic magmas. J. Geol. 87, 509–531.

Anderson Jr., A.T., 1982. Parental basalts in subduction zones: implications for continental evolution. J. Geophys. Res. 87, 7047–7060.

Arculus, R.J., Wills, K.J., 1980. The petrology of plutonic blocks and inclusions from the Lesser Antilles island arc. J. Petrol. 21, 743–799.

Baker, D.R., Eggler, D.H., 1983. Fractionation paths of Atka (Aleutians) high-alumina basalts: constraints from phase relations. J. Volcanol. Geotherm. Res. 18, 387–404.

Baker, D.R., Eggler, D.H., 1987. Compositions of anhydrous and hydrous melts coexisting with plagioclase, augite and olivine or low-Ca pyroxene from 1 atm to 8 kbar: application to the Aleutian volcanic center of Atka. Am. Mineral 72, 12–28.

Beard, J.S., Lofgren, G.E., 1992. An experiment-based model for the petrogenesis of high-alumina basalts. Science 258, 112–115.

Blatter, D.L., Carmichael, I.S.E., 2001. Hydrous phase equilibria of a Mexican high-silica andesite: a candidate for a mantle origin? Geochim. Cosmochim. Acta 65, 4043–4065.

Brophy, J.G., Marsh, B.D., 1986. On the origin of high-alumina basalt and the mechanics of melt extraction. J. Petrol. 27, 763–789.

Clocchiatti, R., Schiano, P., Ottolini, L., Bottazzi, P., 1998. Earlier alkaline and transitional magmatic pulsation of Mt. Etna volcano. Earth Planet. Sci. Lett. 163, 399–407.

Coats, R.R., 1952. Magmatic differentiation in Tertiary and Quaternary volcanic rocks from Adak and Kanaga Islands, Aleutian Islands, Alaska. Bull. Geol. Soc. Am. 63, 485–514.

Conrad, W.K., Kay, R.W., 1984. Ultramafic and mafic inclusions from Adak island: crystallization history, and implications for the nature of primary magmas and crustal evolution in the Aleutian arc. J. Petrol. 25, 88–125.

Conrad, W.K., Kay, S.M., Kay, R.W., 1983. Magma mixing in the Aleutian Arc: evidence from cognate inclusions and composite xenoliths. J. Volcanol. Geotherm. Res. 18, 279–295.

Crawford, A.J., Falloon, T.J., Eggins, S., 1987. The origin of island arc high-alumina basalts. Contrib. Mineral. Petrol. 97, 417–430.

DeBari, S., Kay, S.M., Kay, R.W., 1987. Ultramafic xenoliths from Adagdak volcano, Adak, Aleutian islands, Alaska: deformed igneous cumulates from the Moho of an island arc. J. Geol. 95, 329–341.

Fenner, C.N., 1931. The residual liquids of crystallizing magmas. Mineral. Mag. 22, 539–560.

Gust, D.A., Perfit, M.R., 1987. Phase relations of a high-Mg basalt from the Aleutian Island Arc: implications for primary island arc basalts and high-Al basalts. Contrib. Mineral. Petrol. 97, 7–18.

Himmelberg, G.R., Loney, R.A., 1995. Characteristics and petrogenesis of Alaskan-type ultramafic–mafic intrusions, Southeastern Alaska. U.S. Geol. Surv. Prof. Pap. 1564, 1–47.

Hirose, K., 1997. Melting experiments on lherzolite KLB-1 under hydrous conditions and generation of high-magnesian andesitic melts. Geology 25, 42–44.

Johnston, A.D., 1986. Anhydrous $P-T$ phase relations of near-primary high-alumina basalt from the South Sandwich Islands. Implications for the origin of island arcs and tonalite–trondhjemite series rocks. Contrib. Mineral. Petrol. 92, 368–382.

Kay, R.W., 1980. Volcanic arc magmas: implications of a melting-mixing model for element recycling in the crust–upper mantle system. J. Geol. 88, 497–522.

Kay, S.M., Kay, R.W., 1985a. Aleutian tholeitic and calc-alkaline magma series: I. The mafic phenocrysts. Contrib. Mineral. Petrol. 90, 276–290.

Kay, S.M., Kay, R.W., 1985b. Role of crystal cumulates and the oceanic crust in the formation of the lower crust of the Aleutian arc. Geology 13, 461–464.

Kay, S.M., Kay, R.W., Citron, G.P., 1982. Tectonic controls on tholeiitic and calc–akaline magmatism in the Aleutian Arc. J. Geophys. Res. 87, 4051–4072.

Kelemen, P.B., 1990. Reaction between ultramafic rock and fractionating basaltic magma: I. Phase relations, the origin of calc-alkaline magma series, and the formation of discordant dunite. J. Petrol. 31, 51–98.

Kersting, A.B., Arculus, R.J., 1994. Klyuchevskoy volcano, Kamchatka, Russia: the role of high-flux recharged, tapped and fractionated magma chamber(s) in the genesis of high-Al_2O_3 from high-MgO basalt. J. Petrol. 35, 1–41.

Kushiro, I., 1974. Melting of hydrous upper mantle and possible generation of andesitic magma: an approach from synthetic systems. Earth Planet. Sci. Lett. 22, 294–299.

Marsh, B.D., 1976. Some aleutian andesites: their nature and source. J. Geol. 84, 27–45.

Miyashiro, A., 1974. Volcanic rock series in island arcs and active continental margins. Am. J. Sci. 274, 321–355.

Myers, J.D., 1988. Possible petrogenetic relations between low- and high-MgO Aleutian basalts. Geol. Soc. Amer. Bull. 100, 1040–1053.

Myers, J.D., Frost, C.D., 1994. A petrologic re-investigation of the Adak volcanic center, central Aleutian arc, Alaska. J. Volcanol. Geotherm. Res. 60, 109–146.

Myers, J.D., Marsh, B.D., Sinha, A.K., 1985. Strontium isotopic and selected trace element variations between two Aleutian volcanic centers (Adak and Atka): implications for the development of arc volcanic plumbing systems. Contrib. Mineral. Petrol. 91, 221–234.

Nicholls, I.A., Ringwood, A.E., 1973. Effects of water on olivine stability in tholeiite and the production of silica-saturated magmas in the island arc environment. J. Geol. 81, 285–300.

Nye, C.J., Reid, M.R., 1986. Geochemistry of primary and least-fractionated lavas from Okmok volcano, central Aleutians: implications for arc magmas genesis. J. Geophys. Res. 91, 10271–10287.

O'Hara, M.J., 1968. The bearing of phase equilibria studies in synthetic and natural systems on the origin and evolution of basic and ultrabasic rocks. Earth Sci., Rev. 4, 60–133.

Perfit, M.R., Gust, D.A., Bence, A.E., Arculus, R.J., Taylor, S.R., 1980. Geochemical characteristics of island-arc basalts: implications for mantle sources. Chem. Geol. 30, 227–256.

Presnall, D.C., Dixon, J.R., O'Donnell, T.H., Dixon, S.A., 1979. Generation of mid-ocean ridge tholeiites. J. Petrol. 20, 3–35.

Roedder, E., 1984. Fluid inclusions. In: Ribbe, P.H. (Ed.), Reviews in Mineralogy, vol. 12, pp. 1–644.

Roggensack, K., Williams, S.N., Schaefer, S.J., Parnell Jr., R.A., 1996. Volatiles from the 1994 eruptions of Rabaul: Understanding large caldera systems. Science 273, 490–493.

Schiano, P., Bourdon, B., 1999. On the preservation of mantle information in ultramafic nodules: glass inclusions within minerals versus interstitial glasses. Earth Planet. Sci. Lett. 169, 173–188.

Schiano, P., Eiler, J.M., Hutcheon, I.D., Stolper, E.M., 2000. Primitive CaO-rich, silica-undersaturated melts in island arcs: Evidence for the involvement of clinopyroxene-rich lithologies in the petrogenesis of arc magmas. Geochem. Geophys. Geosyst (G^3) 1, 1–33 (paper number 1999GC000032).

Sisson, T.W., Layne, G.D., 1993. H_2O in basalt and basaltic andesite glass inclusions from four subduction-related volcanoes. Earth Planet. Sci. Lett. 117, 619–635.

Sisson, T.W., Grove, T.L., 1993a. Temperatures and H_2O contents of low-MgO high-alumina basalts. Contrib. Mineral. Petrol. 113, 167–184.

Sisson, T.W., Grove, T.L., 1993b. Experimental investigations of the role of H_2O in calc-alkaline differentiation and subduction zone magmatism. Contrib. Mineral. Petrol. 113, 143–166.

Sobolev, A.V., Barsukov, V.L., Nevsorov, V.N., Slutsky, A.B., 1980. The formation conditions of the high-magnesian olivines from the monominerallic fraction of Luna 24 regolith. Proc. 11th Lunar Sci. Conf. Pergamon, New York, USA, pp. 105–116.

Sobolev, A.V., Shimizu, N., 1993. Ultra-depleted primary melt included in an olivine from the Mid-Atlantic Ridge. Nature 363, 151–154.

Sobolev, A.V., Chaussidon, M., 1996. H_2O concentrations in primary melts from supra-subduction zones and mid-ocean ridges; implications for H_2O storage and recycling in the mantle. Earth Planet. Sci. Lett. 137, 45–55.

Tait, S., 1992. Selective preservation of melt inclusions in igneous phenocrysts. Am. Mineral. 77, 146–155.

Uto, K., 1986. Variations of Al_2O_3 content in Late Cenozoic Japanese basalts: a reexamination of Kuno's High-Alumina Basalts. J. Volcanol. Geotherm. Res. 29, 397–411.

Wyllie, P.J., 1967. Review. In: Wyllie, P.J. (Ed.), Ultramafic and related rocks. Wiley, New York, USA, pp. 403–416.

Yoder, H.S., Tilley, C.E., 1962. Origin of basalt magmas: an experimental study of natural and synthetic rock systems. J. Petrol. 3, 342–532.